Spectrochimica Acta Part A: Molecular and Biomolecular Spectroscopy 230 (2020) 118040

Contents lists available at ScienceDirect

Spectrochimica Acta Part A: Molecular and Biomolecular Spectroscopy

journal homepage: www.elsevier.com/locate/saa

Copper ion modified graphitic C_3N_4 nanosheets enhanced luminol-H_2O_2 chemiluminescence system: Toward highly selective and sensitive bioassay of H_2S in human plasma

Jun-Tao Cao [a,*], Wen-Sheng Zhang [a,c], Xiao-Long Fu [a], Hui Wang [a], Shu-Hui Ma [b], Yan-Ming Liu [a,*]

[a] College of Chemistry and Chemical Engineering, Institute for Conservation and Utilization of Agro-bioresources in Dabie Mountains, Xinyang Normal University, Xinyang 464000, PR China
[b] Xinyang Central Hospital, Xinyang 464000, PR China
[c] Center for Advanced Analytical Science, School of Chemistry and Chemical Engineering, Guangzhou University, Guangzhou 510006, PR China

ARTICLE INFO

Article history:
Received 14 October 2019
Received in revised form 31 December 2019
Accepted 5 January 2020
Available online 7 January 2020

Keywords:
Hydrogen sulfide
Chemiluminescence detection
Copper ion modified graphitic carbon nitride nanosheets

ABSTRACT

A high-efficient chemiluminescence (CL) platform for highly selective and sensitive H_2S detection was constructed on the basis of the quenching effect of S^{2-} on the copper ion modified graphitic carbon nitride nanosheets (Cu^{2+}-g-C_3N_4 NSs) enhanced luminol-H_2O_2 system. Cu^{2+}-g-C_3N_4 NSs with horseradish peroxidase-like catalytic activity were prepared and provide a great improvement for luminol-H_2O_2 system. The presence of S^{2-} induced the formation of CuS precipitate on g-C_3N_4 NSs surface. The precipitate can block the catalytic Cu^{2+} sites on the g-C_3N_4 NSs surface, resulting in a great CL decrease of CL system. Based on such a mechanism, a simple, highly selective and sensitive CL biosensor for H_2S detection was designed. Under the optimized conditions, luminol-H_2O_2-Cu^{2+}-g-C_3N_4 NSs system gave a decrease of CL intensity with the Na_2S concentration increasing. The CL biosensor is in a linear range of 10.0 pM–50.0 nM and the detection limit for detecting Na_2S is as low as 2.0 pM. Moreover, the method here has enjoyed a successful application for determining H_2S in human plasma samples and the recovery is between 95.7% and 110.0%.

1. Introduction

Hydrogen sulfide (H_2S) serves as a gasotransmitter molecule, the same as carbon monoxide (CO) and nitric oxide (NO), can greatly affect the living biosystems [1]. Of these, as a vital signaling molecule, H_2S participates in various physiological activities under physiological conditions, such as vasodilation, oxygen sensing, angiogenesis, apoptosis, neuromodulation and inflammation [2]. Importantly, endogenous H_2S level is correlated with various diseases like Down syndrome, liver cirrhosis, diabetes and Alzheimer's disease [3]. Previous established techniques specific to detecting H_2S mainly are methylene blue method [4], monobromobimane method [5], gas chromatography [6], and sulphide ion selective electrodes [7]. However, some problems including the complicated sample processing, high-cost instruments, as well as low selectivity and sensitivity still puzzled the researchers [8]. Therefore, the development of the selective and sensitive method for H_2S detection on simple setup is highly appealing.

The optical detection techniques can be used to detect volatile gaseous molecule effectively [9]. Fluorescence detection as one of the most popular optical technique has proved its great potential in different biological samples from cell culture to blood serum [10,11]. The strategy by designing the fluorescence probes utilizing Cu^{2+}-fluorophore complex/Cu^{2+}-nanomaterials have been becoming an effective way for H_2S sensing. The mechanism is mainly based on the fluorescent change of the Cu^{2+}-fluorophore complex/Cu^{2+}-nanomaterials in the presence of H_2S owing to the highly affinity of sulfide ions toward Cu ions (K_{sp} of CuS, 1.27×10^{-36}). For example, Sasakura et al. developed an azamacrocyclic Cu^{2+}-complex fluorescent probe for H_2S detection [12]. Zhuo et al. [13] prepared a fluorescent probe of Cu-doped carbon quantum dots to measure H_2S in human serum and image H_2S in living cells. However, fluorescent probes always suffer from the poor photostability and are prone to photobleaching and photodegradation, limiting their further applications. To avoid the phenomenon, chemiluminescence (CL) should be a good choice with the features of no need of excitation source, low background nature, simple equipment and high sensitivity. Inspired by the above mentioned examples, is it possible to introduce the Cu^{2+} mediated mechanism into the CL system to improve the CL performance for H_2S detection?

In many CL systems, e.g., luminol-H_2O_2 [14], N-aminobutyl-N-ethylisoluminol functionalized graphene oxide-H_2O_2 [15], nitrogen and sulfur co-doped carbon dots-H_2O_2 [16], in which horseradish

* Corresponding authors.
E-mail addresses: jtcao11@163.com (J.-T. Cao), liuym9518@sina.com (Y.-M. Liu).

https://doi.org/10.1016/j.saa.2020.118040
1386-1425/

peroxidases (HRP) are always adopted as a catalyst for the enhancement of CL intensity. With the development of nanoscience and nanotechnology, the nanomaterials with excellent catalytic effect have been synthesized to mimic the horseradish peroxidase (HRP) functions like iron oxide [17], Au [18], or Cu [19] nanoparticles. Recently, Vázquez-González et al. reported that the Cu^{2+}-modified graphitic carbon nitride nanoparticles (Cu^{2+}-g-C_3N_4 NPs) featured the HRP biocatalytic functions [20]. In this work, by integrating the unique function of Cu^{2+}-g-C_3N_4 NPs with high affinity of S^{2-} toward Cu^{2+}, a simple, highly selective and sensitive CL platform for H_2S detection was proposed in virtue of the quenching effect of H_2S on the Cu^{2+}-g-C_3N_4 nanosheets (Cu^{2+}-g-C_3N_4 NSs) enhanced luminol-H_2O_2 system. According to Scheme 1, thanks to the catalysis of Cu^{2+}-g-C_3N_4 to luminol-H_2O_2, the system exhibits a strong CL emission. Upon the addition of Na_2S (employed as the H_2S donor), the CuS precipitate formed on the Cu^{2+}-g-C_3N_4 NSs surface and thus the CL intensity declined. The proposed method allowed for the detection of H_2S in a sensitive manner. Moreover, the CL biosensor was applied for determination H_2S in human plasma samples.

2. Experimental

2.1. Materials and Reagents

Glutathione (GSH), homocysteine (Hcy), L-cysteine (Cys) and melamine were purchased from the Aladdin Industrial Co., Ltd. (Shanghai, China). Glycine (Gly) was bought from the Seebio Biotechnology Co., Ltd. (Shanghai, China). Serine (Ser), alanine (Ala), L-lysine (Lys), sodium nonasulfate ($Na_2S•9H_2O$), zinc sulfate ($ZnSO_4$), ferrous sulfate ($FeSO_4$), copper sulfate ($CuSO_4$), calcium chloride ($CaCl_2$), Ferric chloride ($FeCl_3$), ascorbic acid (AA), nitric acid (HNO_3) and citric acid (CA) were provided by the Sinopharm Chemical Reagent Co., Ltd. (Shanghai, China). 1.0×10^{-2} M luminol stock solution was used to prepare the luminol working solution. Other AR-grade reagents were used directly. All aqueous solutions were prepared by pure water (18.2 MΩ·cm) obtained from the ultrapure water system (Aike Water Treatment Solution Provider, China).

2.2. Apparatus

CL measurements were performed on an ultra-weak luminescence analyzer (BPCL-1-TIC, Institute of Biophysics, Chinese Academy of Science, Beijing, China). The CL emission was recorded on the F-7000 fluorescence and UV–vis absorption spectra were recorded on the U—3900H UV–vis spectrophotometer (Hitachi, Tokyo, Japan). A Tecnai G2 F20 S-TWIN microscope (FEI Co., Ltd., USA) was applied for the Transmission electron microscopy (TEM), the scanning-TEM energy dispersive X-ray spectroscopy (STEM-EDS) as well as the STEM-mapping. A KAlpha X-ray photoelectron spectrometer (Thermo Fisher Scientific Co., USA) was employed to perform X-ray photoelectron spectroscopy (XPS) and a FTIR-8400S spectrometer (Shimadzu, Japan) helped to perform the Fourier transform infrared (FT-IR) spectroscopy.

2.3. Cu^{2+}-g-C_3N_4 NSs Preparation

The preparation of the g-C_3N_4 NSs was conducted following the reported methods [21,22] and there was a little improvement. At first, 5.0 g white melamine powders received 4 h annealing at 550 °C to acquire the yellow bulk g-C_3N_4. Second, a certain amount of the bulk g-C_3N_4 product (600 mg) were ground to a powder form and transferred to 200 mL of 5.0 M HNO_3. Then the mixture underwent 1 h sonicate. Next, the produced solution was refluxed at 125 °C for 12 h. After cooled to the room temperature, the reaction product underwent centrifugation treatment, and then water was used to wash it to near-neutral pH. Subsequently, the obtained g-C_3N_4 nanoflakes of the previous step were transferred to 60 mL of water for exfoliation, which was kept for 16 h under ultrasound. Finally, the centrifugation at 8000 rpm for 10 min was conducted for discard of the unexfoliated g-C_3N_4. The collected suspension with g-C_3N_4 NSs was dried at 60 °C for later use.

The Cu^{2+}-g-C_3N_4 NSs were synthesized as follows: In brief, a certain amount of g-C_3N_4 NSs (20.0 mg) was dissolved in 20 mL pure water for 10 min by ultrasonication. Then, the formed solution was added with 20.0 mL 0.05 M $CuCl_2$ (The optimization of the $CuCl_2$ concentration, see the section of 3.2). Following 4 h sonication at 80 °C, the mixture underwent centrifugation treatment and wash three times by pure water for the removal of excess $CuCl_2$. Finally, the product was dried for further use.

2.4. Construction of the CL Biosensor

The ingenious CL biosensor was constructed based on the probe of Cu^{2+}-g-C_3N_4 NSs-triggered strong CL response of luminol-H_2O_2 system. As displayed in Scheme 1, for H_2S detection, a series of various concentrations of Na_2S (using Na_2S as the equivalent [23]) was added into the Cu^{2+}-g-C_3N_4 NSs suspension, followed by 30 min incubation. The portion of Cu^{2+}-g-C_3N_4 NSs was first centrifuged and then washed using phosphate buffer solution, followed by being reacted with dissociated S^{2-} to form CuS-g-C_3N_4 NSs for CL assay.

3. Results and Discussion

3.1. Characterization of g-C_3N_4 NSs and Cu^{2+}-g-C_3N_4 NSs

TEM was performed to characterize the prepared Cu^{2+}-g-C_3N_4 and g-C_3N_4 NSs. According to Fig. 1A and B, pure g-C_3N_4 NSs and Cu^{2+}-g-C_3N_4 NSs present analogous laminated structure, which indicates basically no change in the basic morphology following Cu^{2+}-doping. Meanwhile, the TEM image also demonstrates that Cu^{2+}-g-C_3N_4 NSs are relatively thin with a high transparency. Then, the STEM-EDS spectrum (Fig. 1C) confirms that the Cu^{2+}-g-C_3N_4 NSs are composed of the

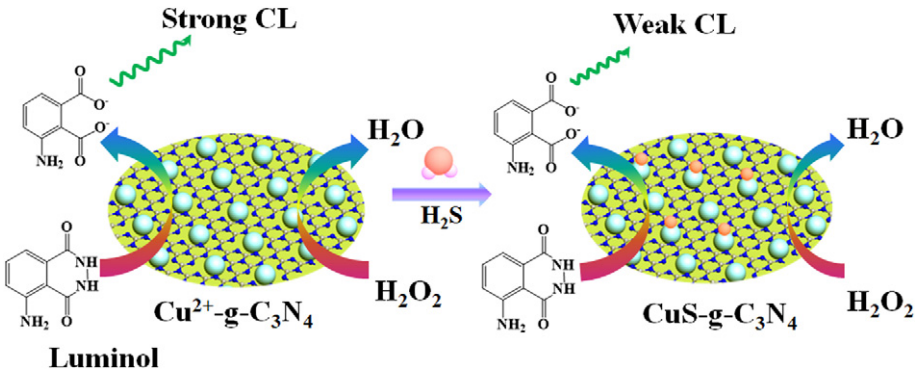

Scheme 1. Schematic illustration of CL assay of H_2S.

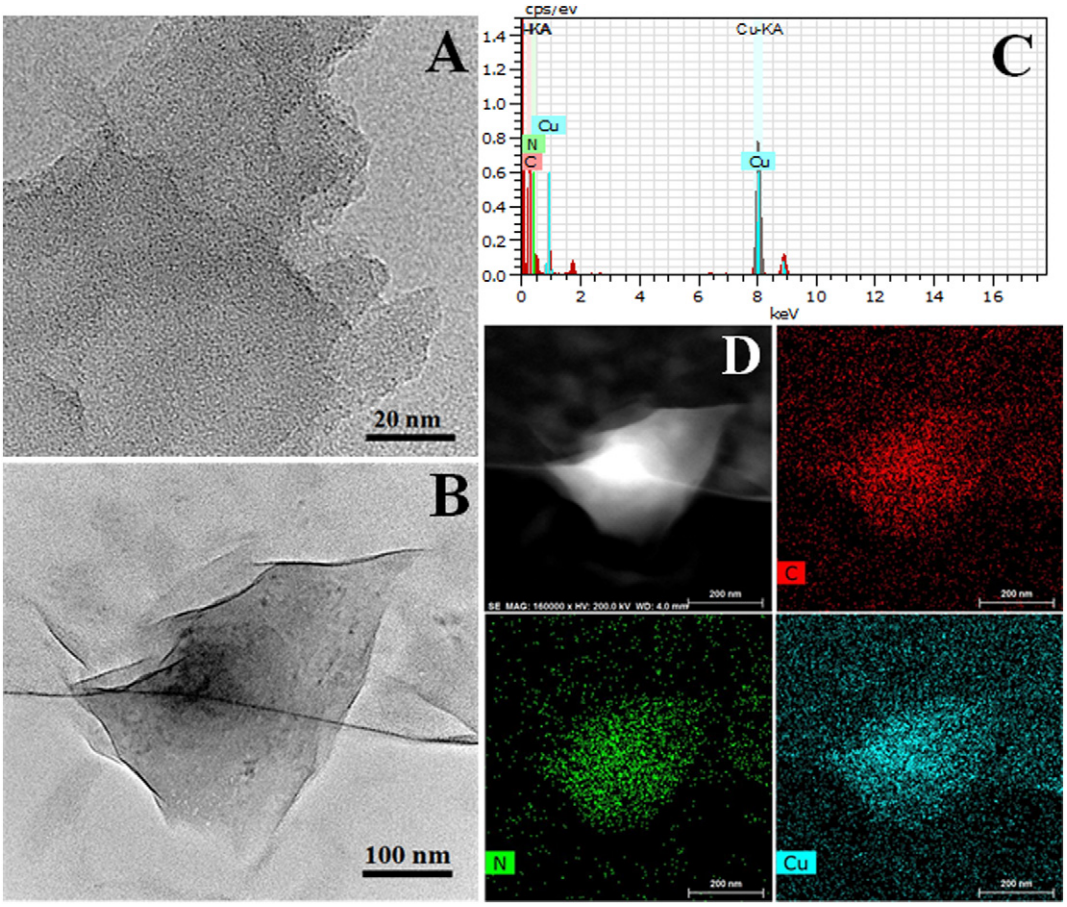

Fig. 1. TEM images of g-C_3N_4 NSs (A), Cu^{2+}-g-C_3N_4 NSs (B) and the STEM-EDS image of Cu^{2+}-g-C_3N_4 NSs (C) and the EDS elemental mappings of C, N and Cu elements for Cu^{2+}-g-C_3N_4 NSs (D).

elements C, N, and Cu. Element mapping characterizations were implemented to further explore the structure of the prepared Cu^{2+}-g-C_3N_4 NSs. Fig. 1D displays that, the STEM-mapping clearly exhibit the identical distribution of C, N, and Cu elements in the Cu^{2+}-g-C_3N_4 NSs (Fig. 1D). These data prove the successful preparation of Cu^{2+}-g-C_3N_4 NSs.

The surface groups, structures and components of Cu^{2+}-g-C_3N_4 NSs were further studied by FT-IR, UV–vis and XPS spectra. It can be seen from the FT-IR spectra in Fig. 2A that the graphitic C—N network does not change obviously after Cu^{2+} doping in g-C_3N_4 NSs (curves a and b). The peak at 804 cm^{-1} was caused by the breathing mode regarding the triazine units [24,25]. The peaks ranging from 1200 cm^{-1} to 1700 cm^{-1} act as typical aromatic C—N stretching modes, thereinto, the peaks at 1250 cm^{-1} is assigned as the stretching vibration of C—N, and the other two peaks at 1413 cm^{-1}, and 1635 cm^{-1} are assigned as the stretching modes of heptazine-derived units [26,27]. Broad peaks from 3000 cm^{-1} to 3500 cm^{-1} originate from the stretching vibration of the N—H and the O—H, which indicate the existence of physical adsorbed water and amino groups in both g-C_3N_4 NSs and Cu^{2+}-g-C_3N_4 NSs. A new peak appears at about 1054 cm^{-1} after Cu doping, which could be caused by the stretching vibration of the C—N in the copper phthalocyanine molecule [26]. There is an obvious absorption band (~325 nm) in the UV–vis absorption spectra for both samples (curves a: g-C_3N_4 NSs, and curve b: Cu^{2+}-g-C_3N_4 NSs), which correspond to the electronic transition from valence band to conduction band (Fig. 2B). After being added with Cu^{2+}, absorption band shows a partial red shift (~5 nm) because of the enhancement of the photocatalytic property in the visible area, which is related with the typical semiconductor absorption of g-C_3N_4 substrate.

In addition, XPS analysis was accomplished to analyze the elemental composition of the synthesized Cu^{2+}-g-C_3N_4 NSs in detail (Fig. 2C). The XPS survey spectra show several visible peaks at 23.2 eV (O2s), 207.1 eV (Cl2p), 291.6 eV (Cls), 408.6 eV (N1 s), 540.6 eV (O1s), 959.1 eV (Cu2p) and 980.4 eV (OKLL) [28]. Furthermore, the XPS data verified the existence of the carbon (46.22%), nitrogen (45.62%), oxygen (5.53%), copper (1.34%), and chlorine (1.29%) in Cu^{2+}-g-C_3N_4 NSs. That is, the XPS indicated the coverage of Cu^{2+} ions corresponding to about 0.0134 mg per 1.0 mg of Cu^{2+}-g-C_3N_4 NSs. All the data validate that Cu^{2+}-g-C_3N_4 NSs were successfully synthesized.

3.2. Optimization of CL Working Conditions

To achieve excellent analytical performance, the concentrations of luminol, H_2O_2, Cu^{2+}-g-C_3N_4 NSs, and $CuCl_2$ used for g-C_3N_4 NSs modification needed to be optimized. The effect of luminol concentration ranged from 0.25 to 5.0 mM on the CL signal response was tested. The luminol concentration increase from 0.25 to 1.5 mM helped to significantly enhance the CL intensity (Fig. S1A). However, as the luminol concentration further increased, the CL intensity decreased. Therefore, 1.5 mM luminol was chosen. As the coreactant of luminol, H_2O_2 concentration was also screened. As depicted in Fig. S1B, the CL intensity increased as the H_2O_2 concentration increased and reached a plateau at 2.0 mM. Hence, 2.0 mM H_2O_2 was selected.

As a catalyst mimicking the HRP, Cu^{2+}-g-C_3N_4 NSs possessed the biocatalytic function to luminol-H_2O_2 system. To screen the appropriate concentration of Cu^{2+}-g-C_3N_4 NSs, the concentration from 0.05 to 4.0 mg mL^{-1} was tested. As shown in Fig. S1C, the CL intensity increased to a maximum value at 0.5 mg mL^{-1}. Therefore, 0.5 mg mL^{-1} was used.

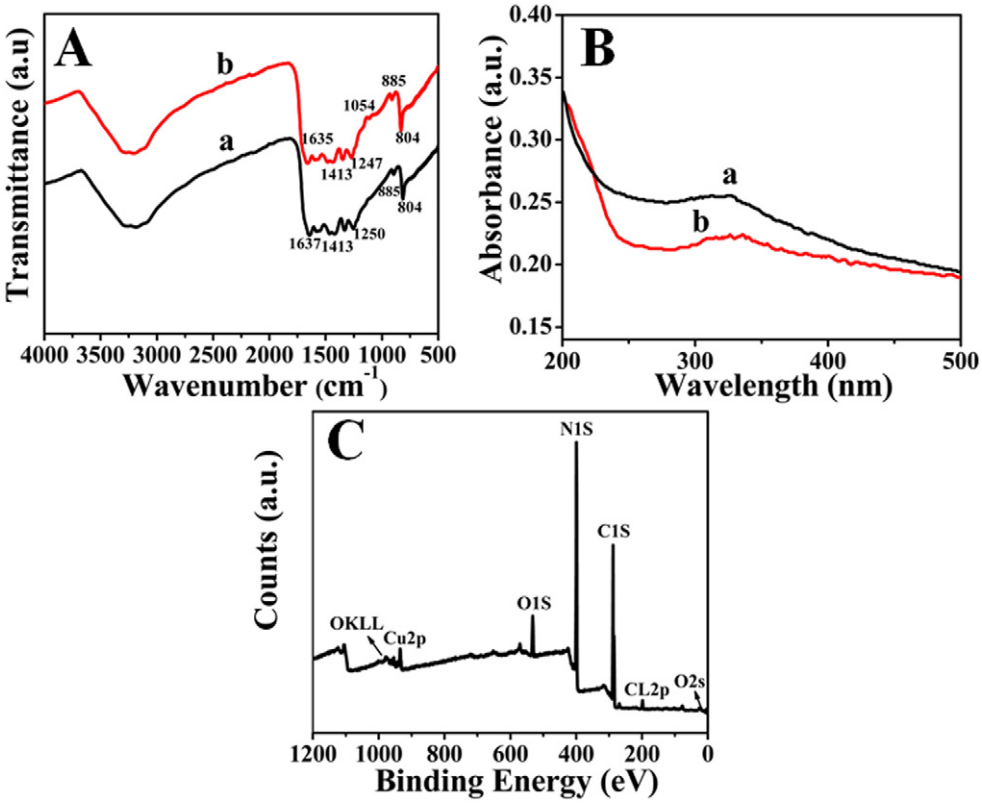

Fig. 2. FT-IR (A) and UV–vis spectra (B) obtained for g-C_3N_4 NSs (a), and Cu^{2+}-g-C_3N_4 NSs (b). (C) XPS spectra of Cu^{2+}-g-C_3N_4 NSs.

To ensure that the Cu^{2+}-g-C_3N_4 NSs exhibit a highly catalytic function toward luminol-H_2O_2 system, the CL of the Cu^{2+}-g-C_3N_4 NSs with the variable concentrations of $CuCl_2$ (0–0.2 M) at fixed amount of g-C_3N_4 NSs (0.1 mg mL^{-1} g-C_3N_4 suspension) were recorded. As shown in Fig. S1D, the modification of Cu^{2+} on the g-C_3N_4 NSs surface (curve b-g) could remarkably improve the system's CL intensity compared with the pure g-C_3N_4 NSs (curve a), indicating the vital catalytic role of coordinated Cu^{2+} in Cu^{2+}-g-C_3N_4 NSs [25]. The CL intensity increased with the $CuCl_2$ concentration increasing until 0.05 M (curve a–e). The concentration beyond 0.05 M gives no obvious CL change, which could be ascribed to the saturated loading of Cu^{2+} on g-C_3N_4 NSs surface. Based on the above analysis, the 0.05 M concentration of $CuCl_2$ was selected for probe synthesis.

3.3. Possible Mechanism

To investigate the catalytic property of Cu^{2+}-g-C_3N_4 NSs on luminol-H_2O_2 system, a series of experiments were designed. Fig. 3A depicts the CL kinetics curves of different CL systems. As shown, the CL signal of the luminol-H_2O_2 system is very weak (curve a), and the separated addition of Cu^{2+} (1.05×10^{-4} M) or g-C_3N_4 NSs could promote CL signals (curves b and c), suggesting the Cu^{2+} and g-C_3N_4 NSs have certain catalytic activity toward the luminol-H_2O_2 system, respectively. Upon the introduction of Cu^{2+}-g-C_3N_4 NSs into luminol-H_2O_2 system, a sharp and strong CL response was observed (curve d).

To further explore the CL mechanism of the luminol-H_2O_2-Cu^{2+}-g-C_3N_4 NSs system, the CL spectra of different systems were measured by the fluorescence spectrometer by taking off the light source. As

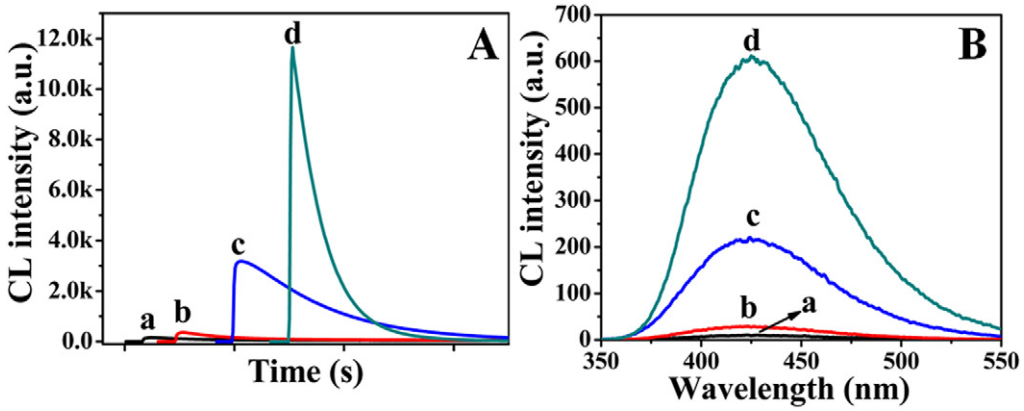

Fig. 3. CL kinetics curves (A) of and CL spectra (B) of luminol-H_2O_2 (a), luminol-H_2O_2-Cu^{2+} ($C_{Cu2+} = 1.05 \times 10^{-4}$ M) (b), luminol-H_2O_2-g-C_3N_4 NSs (c), and luminol-H_2O_2-Cu^{2+}-g-C_3N_4 NSs (d).

displayed in Fig. 3B, the emission peaks of the luminol-H_2O_2, luminol-H_2O_2-Cu^{2+}, luminol-H_2O_2-g-C_3N_4 NSs, and luminol-H_2O_2-Cu^{2+}-g-C_3N_4 NSs are all around 425 nm. These data reveals that the luminescent species in these systems are excited luminol [29,30], and the signal enhancement trend of CL spectrum is consistent with the CL kinetic behavior. Based on the above analysis, combining with the previously reported catalytic mechanism of Cu^{2+} on luminol-H_2O_2 system [31,32] and the CL reaction process of g-C_3N_4 NSs-based system [33,34]. The possible luminescent mechanism of the luminol-H_2O_2-Cu^{2+}-g-C_3N_4 NSs system could be described by the following equations:

$$H_2O_2 + Cu^{2+}\text{-g-}C_3N_4 \xrightarrow{OH^-} Cu^{+}\text{-}{}^{\cdot}\text{g-}C_3N_4^{-} + {}^{\cdot}O_2^{-} + HO_2^{-} + H_2O \quad (1)$$

$$H_2O_2 + Cu^{+}-{}^{\bullet}g-C_3N_4^{-} \rightarrow Cu^{2+}-g-C_3N_4 + {}^{\bullet}OH + OH^{-} \quad (2)$$

$$\text{Luminol} + {}^{\bullet}OH \rightarrow \text{luminol radicals } (L^{\bullet -}) \quad (3)$$

$$\text{Luminol radicals } (L^{\bullet -}) + {}^{\bullet}O_2^{-} \rightarrow \text{hydroxyl hydroperoxide } (LOO^{-}) + N_2 + h\nu \quad (4)$$

3.4. Analytical Performance

To demonstrate the feasibility of Cu^{2+}-g-C_3N_4 NSs as probes for H_2S sensing, Na_2S with varied concentrations were tested. The results showed that CL signal changed proportionally with Na_2S concentration in logarithmic scale in the range of 10.0 pM–50.0 nM (Fig. 4A). The reason for this is that the enhanced concentration of Na_2S could result in the increased amount of CuS formed on g-C_3N_4 NSs surface, blocking catalytic Cu^{2+} sites on the surface of the g-C_3N_4 NSs. Fig. 4B depicts that the CL intensity is linearly related to the logarithm of Na_2S concentration, which follows the regression equation $I = -3378.02 - 1286.92 \log C$ (C represents the concentration of S^{2-}, $R^2 = 0.997$). The detection limit is found to be 2.0 pM (S/N = 3). Moreover, the proposed method was compared with the previously reported method for detecting H_2S. For the well-designed biosensor, the linear range was relatively wide and the detection limit was low for H_2S detection (Table 1).

3.5. Specificity, Stability, and Precision

For evaluating the selectivity of the CL biosensor, some possible interfering species such as metal ions, amino acids, biothiols and CA, glucose and AA were examined. As shown in Fig. S2A, the existence of 100 μM of Na^+, K^+, Mg^{2+}, Gly, Ser, Lys, CA, Gluocose, Ala and AA, led to scarcely change of the CL signal, whereas 50.0 nM Na_2S could result in an obvious CL decrease. The other interferences such as Fe^{3+}, Cu^{2+}, Zn^{2+}, Fe^{2+}, Hcy, Cys, and GSH (each of 100 μM) caused a slight change of CL response, and the corresponding signal fluctuation rate of CL was calculated as $\Delta I/I_{blank}$ values, i.e., $(I_{Fe3+} - I_{blank})/I_{blank} = 3.2\%$, $(I_{Cu2+} - I_{blank})/I_{blank} = 3.3\%$, $(I_{Zn2+} - I_{blank})/I_{blank} = 2.8\%$, $(I_{Fe2+} - I_{blank})/I_{blank} = 2.9\%$, $(I_{Hcy} - I_{blank})/I_{blank} = -2.6\%$, $(I_{Cys} - I_{blank})/I_{blank} = -3.5\%$, $(I_{GSH}\text{-}I_{blank})/I_{blank} = -4.4\%$ are all less than ±5%. Therefore, the results exhibited that the method has good selectivity for H_2S detection.

Table 1
Comparison of the proposed method and the referenced methods for H_2S detection.

Methods	Linear ranges	LODs	References
PEC method	10.0 nM–1.0 mM	0.31 nM	[35]
FL probe	1.0 μM–10.0 μM	0.12 μM	[36]
Multicolor colorimetric assay	0.05 μM–50.0 μM	19.0 nM	[37]
Smart colorimetric probe	0.7 μM–10.0 μM	0.2 μM	[38]
Ultrasensitive PEC sensor	1.0 pM–10.0 nM	0.36 pM	[39]
CL biosensor	10.0 pM–50.0 nM	2.0 pM	This work

The CL response of the Cu^{2+}-g-C_3N_4 NSs probe with various storage times (0 week, 1 week, 2 weeks and 3 weeks) for 50.0 nM Na_2S was recorded to examine the stability of the system. As demonstrated in Fig. S2B, the difference in CL intensity is negligible within 3 weeks, indicating that the system presents an acceptable stability.

The assay of 50.0 nM Na_2S for 6 parallel measurements within one day and three days was carried out to estimate the intra-assay precision and inter-assay precision. The relative standard deviations (RSDs) for intra-assay were no more than 3.5%, while the RSDs for inter-assay were less than 6.3%.

3.6. Analytical Applications

To verify the applicability of the system, the content of sulphide in healthy human plasma (provided by Xinyang Central Hospital) were determined. Prior to analysis, the fresh human plasma samples are properly diluted and pretreated as the follows: briefly, acetonitrile was added into human plasma (7:1 v/v plasma/acetonitrile) to remove the proteins [40]; After centrifugated for 10 min at 10000 rpm, the resultant supernatant was immediately used for analysis. As listed in Table S1, the sulphide concentration of the plasma averaged at 0.47 ± 0.04 μM from three healthy individuals, which were basically consistent with the reported methods [8,40]. In addition, the recovery experiments were executed by spiking Na_2S (0.2 and 0.4 μM) into three human plasma samples, respectively. The recoveries vary from 95.7% to 110.0%, and the RSDs are no more than 6.1%, indicating that the method has a good accuracy for the detection of H_2S in the biological samples.

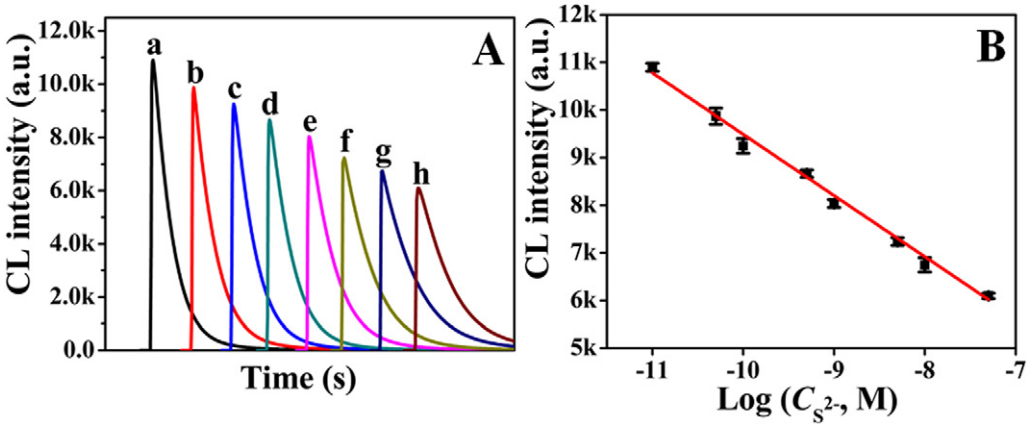

Fig. 4. (A) CL signal responses of different concentrations of Na_2S: (a) 10.0 pM, (b) 50.0 pM, (c) 100.0 pM, (d) 500.0 pM, (e) 1.0 nM, (f) 5.0 nM, (g) 10.0 nM and 50.0 nM. (B) The linear plot between CL intensity and the logarithm of Na_2S concentration.

4. Conclusions

In summary, the study developed a CL biosensor for detecting H_2S on the basis of the quenching effects of H_2S on Cu^{2+}-g-C_3N_4 NSs enhanced luminol-H_2O_2 system. Cu^{2+}-g-C_3N_4 NSs exhibit excellent catalytic activity to luminol-based system. By virtue of the blocking effects of S^{2-} to catalytic Cu^{2+} sites on the surface of the g-C_3N_4 NSs, the presence of H_2S produce a great signal decline of the Cu^{2+}-g-C_3N_4 NSs-luminol-H_2O_2 system. Hence, the constructed CL system presents a high sensitivity and good selectivity for detecting H_2S. The CL biosensor has been applied to determining H_2S in human plasma samples, providing a new promising method for sensitive detection of H_2S in biofluids.

Credit Author Statement

Jun-Tao Cao: Conceptualization, Methodology, Supervision, Project administration, Writing-original draft, Writing-review & editing. **Wen-Sheng Zhang:** Conceptualization, Methodology, Investigation, Writing-original draft. **Xiao-Long Fu:** Investigation. **Hui Wang:** Supervision. **Shu-Hui Ma:** Validation. **Yan-Ming Liu:** Conceptualization, Methodology, Supervision, Project administration, Writing-original draft, Writing-review & editing.

Declaration of Competing Interest

The authors declare that they have no known competing financial interests or personal relationships that could have appeared to influence the work reported in this paper.

Acknowledgements

This work was supported by the National Natural Science Foundation of China (Grant No. 21675136 and 21874115), Science & Technology Innovation Talents in Universities of Henan Province (18HASTIT003), and Nanhu Scholars Program for Young Scholars of XYNU.

Appendix A. Supplementary Data

Supplementary data to this article can be found online at https://doi.org/10.1016/j.saa.2020.118040.

References

[1] M.D. Hartle, M.D. Pluth, A practical guide to working with H_2S at the interface of chemistry and biology, Chem. Soc. Rev. 45 (2016) 6108–6117.
[2] J.P. Collman, S. Ghosh, A. Dey, R.A. Decréau, Using a functional enzyme model to understand the chemistry behind hydrogen sulfide induced hibernation, P. NATL. ACAD. SCI USA 106 (2009) 22090–22095.
[3] P. Kamoun, M.C. Belardinelli, A. Chabli, K. Lallouchi, B. Chadefaux-Vekemans, Endogenous hydrogen sulfide overproduction in Down syndrome, Am. J. Med. Genet. A 116 (2003) 310–311.
[4] M.N. Hughes, M.N. Centelles, K.P. Moore, Making and working with hydrogen sulfide: the chemistry and generation of hydrogen sulfide in vitro and its measurement in vivo: a review, Free Radical Bio. Med. 47 (2009) 1346–1353.
[5] X.G. Shen, C.B. Pattillo, S. Pardue, S.C. Bir, R. Wang, C.G. Kevil, Measurement of plasma hydrogen sulfide in vivo and in vitro, Free Radical Bio. Med. 50 (2011) 1021–1031.
[6] P.R. Bérubé, P.D. Parkinson, E.R. Hall, Measurement of reduced Sulphur compounds contained in aqueous matrices by direct injection into a gas chromatograph with a flame photometric detector, J. Chromatogr. A 830 (1999) 485–489.
[7] A. Faccenda, J.Y. Wang, B. Mutus, Polydimethylsiloxane permeability-based method for the continuous and specific detection of hydrogen sulfide, Anal. Chem. 84 (2012) 5243–5249.
[8] X.G. Shen, E.A. Peter, S. Bir, R. Wang, C.G. Kevil, Analytical measurement of discrete hydrogen sulfide pools in biological specimens, Free Radical Bio. Med. 52 (2012) 2276–2283.
[9] B. Ke, W.X. Wu, W. Liu, H. Liang, D.Y. Gong, X.T. Hu, M.Y. Li, Bioluminescence probe for detecting hydrogen sulfide in vivo, Anal. Chem. 88 (2015) 592–595.
[10] Y. Qian, J. Karpus, O. Kabil, S.Y. Zhang, H.L. Zhu, R. Banerjee, C. He, Selective fluorescent probes for live-cell monitoring of sulphide, Nat. Commun. 2 (2011) 495.
[11] J. Cao, R. Lopez, J.M. Thacker, J.Y. Moon, C. Jiang, S.N.S. Morris, A.R. Lippert, Chemiluminescent probes for imaging H_2S in living animals, Chem. Sci. 6 (2015) 1979–1985.
[12] K. Sasakura, K. Hanaoka, N. Shibuya, Y. Mikami, Y. Kimura, T. Komatsu, T. Nagano, Development of a highly selective fluorescence probe for hydrogen sulfide, J. Am. Chem. Soc. 133 (2011) 18003–18005.
[13] S.J. Zhuo, L.L. Gao, P. Zhang, J.Y. Du, C.Q. Zhu, Living cell imaging and sensing of hydrogen sulfide using high-efficiency fluorescent Cu-doped carbon quantum dots, New J. Chem. 42 (2018) 19659–19664.
[14] A.N. Díaz, F.G. Sanchez, J.G. García, Hydrogen peroxide assay by using enhanced chemiluminescence of the luminol-H_2O_2-horseradish peroxidase system: comparative studies, Anal. Chim. Acta 327 (1996) 161–165.
[15] X. Liu, Z. Han, F. Li, L. Gao, G. Liang, H. Cui, Highly chemiluminescent graphene oxide hybrids bifunctionalized by N-(aminobutyl)-N-(ethylisoluminol)/horseradish peroxidase and sensitive sensing of hydrogen peroxide, ACS Appl. Mater. Interfaces 7 (2015) 18283–18291.
[16] J.T. Cao, W.S. Zhang, H. Wang, S.H. Ma, Y.M. Liu, A novel nitrogen and sulfur co-doped carbon dots-H_2O_2 chemiluminescence system for carcinoembryonic antigen detection using functional HRP-Au@Ag for signal amplification, Spectrochim. Acta, Part A 219 (2019) 281–287.
[17] R. Schlögl, Heterogeneous catalysis, Angew. Chemie Int. Ed. 54 (2015) 3465–3520.
[18] Y. Zhao, Y. Huang, H. Zhu, Q. Zhu, Y. Xia, Three-in-one: sensing, self-assembly, and cascade catalysis of cyclodextrin modified gold nanoparticles, J. Am. Chem. Soc. 138 (2016) 16645–16654.
[19] M.B. Gawande, A. Goswami, F.X. Felpin, T. Asefa, X. Huang, R. Silva, R.S. Varma, Cu and Cu-based nanoparticles: synthesis and applications in catalysis, Chem. Rev. 116 (2016) 3722–3811.
[20] M. Vázquez-González, W.C. Liao, R. Cazelles, S. Wang, X. Yu, V. Gutkin, I. Willner, Mimicking horseradish peroxidase functions using Cu^{2+}-modified carbon nitride nanoparticles or Cu^{2+}-modified carbon dots as heterogeneous catalysts, ACS Nano 11 (2017) 3247–3253.
[21] X.D. Zhang, X. Xie, H. Wang, J.J. Zhang, B.C. Pan, Y. Xie, Enhanced photoresponsive ultrathin graphitic-phase C_3N_4 nanosheets for bioimaging, J. Am. Chem. Soc. 135 (2012) 18–21.
[22] L.C. Chen, D.J. Huang, S.Y. Ren, T.Q. Dong, Y.W. Chi, G.N. Chen, Preparation of graphite-like carbon nitride nanoflake film with strong fluorescent and electrochemiluminescent activity, Nanoscale 5 (2013) 225–230.
[23] Y. Qian, L. Zhang, S.T. Ding, X. Deng, C. He, X.E. Zheng, J. Zhao, A fluorescent probe for rapid detection of hydrogen sulfide in blood plasma and brain tissues in mice, Chem. Sci. 3 (2012) 2920–2923.
[24] P.L. Cook, W. Yang, X. Liu, J.M. García-Lastra, A. Rubio, F.J. Himpsel, Unoccupied states in Cu and Zn octaethyl-porphyrin and phthalocyanine, J. Chem. Phys. 134 (2011), 204707.
[25] H.L. Dou, L. Chen, S.H. Zheng, Y.P. Zhang, G.Q. Xu, Band structure engineering of graphitic carbon nitride via Cu^{2+}/Cu^{+} doping for enhanced visible light photoactivity, Mater. Chem. Phys. 214 (2018) 482–488.
[26] S. Singh, S.K. Tripathi, G.S.S. Saini, Optical and infrared spectroscopic studies of chemical sensing by copper phthalocyanine thin films, Mater. Chem. Phys. 112 (2008) 793–797.
[27] L. Chen, Y.H. Man, Z.Q. Chen, Y.P. Zhang, Ag/g-C_3N_4 layered composites with enhanced visible light photocatalytic performance, Mater. Res. Express 3 (2016), 115003.
[28] Y. Lin, P. Kannan, Y.B. Zeng, B. Qiu, L.H. Guo, Z.Y. Lin, Enzyme-free multicolor biosensor based on Cu^{2+}-modified carbon nitride nanosheets and gold nanobipyramids for sensitive detection of neuron specific enolase, Sensor Actuators B-Chem 283 (2019) 138–145.
[29] M. Zhang, X.Q. Xiao, W.Y. Zeng, X.Y. Zeng, H.C. Yao, Determination of 2-methoxyestradiol in serum samples and pharmaceutical preparations by silver nanoparticles-enhanced chemiluminescence, Talanta 120 (2014) 331–335.
[30] W.S. Zhang, J.T. Cao, Y.X. Dong, H. Wang, S.H. Ma, Y.M. Liu, Enhanced chemiluminescence by Au-Ag core-shell nanoparticles: a general and practical biosensing platform for tumor marker detection, J. Lumin. 201 (2018) 163–169.
[31] M.J. Chaichi, S.O. Alijanpour, Chitosan-induced Au/Ag nanoalloy dispersed in IL and application in fabricating an ultrasensitive glucose biosensor based on luminol-H_2O_2-Cu^{2+}/IL chemiluminescence system, J. Photoch. Photobio. B-Bio. 140 (2014) 41–48.
[32] S. Bi, H. Zhou, S.S. Zhang, A novel synergistic enhanced chemiluminescence achieved by a multiplex nanoprobe for biological applications combined with dual-amplification of magnetic nanoparticles, Chem. Sci. 1 (2010) 681–687.
[33] Y.Z. Zheng, X.N. Dou, H.F. Li, J.M. Lin, Bisulfite induced chemiluminescence of g-C_3N_4 nanosheets and enhanced by metal ions, Nanoscale 8 (2016) 4933–4937.
[34] L.L. Ding, J.P. Ge, W.Q. Zhou, J.P. Gao, Z.Y. Zhang, Y. Xiong, Nanogold-functionalized g-C_3N_4 nanohybrids for sensitive impedimetric immunoassay of prostate-specific antigen using enzymatic biocatalytic precipitation, Biosens. Bioelectron. 85 (2016) 212–219.
[35] H. Li, Y. Tian, Z.F. Deng, Y. Liang, An in situ photoelectrochemical determination of hydrogen sulfide through generation of CdS nanoclusters onto TiO_2 nanotubes, Analyst 137 (2012) 4605–4609.
[36] Z. Xu, L. Xu, J. Zhou, Y.F. Xu, W.P. Zhu, X.H. Qian, A highly selective fluorescent probe for fast detection of hydrogen sulfide in aqueous solution and living cells, Chem. Commun. 48 (2012) 10871–10873.
[37] Z.H. Chen, C.Q. Chen, H.W. Huang, F. Luo, L.H. Guo, L. Zhang, Z.Y. Lin, G.N. Chen, Target-induced horseradish peroxidase deactivation for multicolor colorimetric assay of hydrogen sulfide in rat brain microdialysis, Anal. Chem. 90 (2018) 6222–6228.
[38] Y. Zhang, H.Y. Shen, X. Hai, X.W. Chen, J.H. Wang, Polyhedral oligomeric silsesquioxane polymer-caged silver nanoparticle as a smart colorimetric probe for the detection of hydrogen sulfide, Anal. Chem. 89 (2016) 1346–1352.
[39] H.B. Li, J. Li, Y.Y. Zhu, W.Y. Xie, R. Shao, X.X. Yao, A.Q. Gao, Y.D. Yin, Cd^{2+}-doped amorphous TiO_2 hollow spheres for robust and ultrasensitive photoelectrochemical sensing of hydrogen sulfide, Anal. Chem. 90 (2018) 5496–5502.
[40] L. Zhang, S. Li, M. Hong, Y.Q. Xu, S.S. Wang, Y. Liu, J. Zhao, A colorimetric and ratiometric fluorescent probe for the imaging of endogenous hydrogen sulphide in living cells and sulphide determination in mouse hippocampus, Org. Biomol. Chem. 12 (2014) 5115–5125.